HHS Public Access

Author manuscript

Mol Cancer Ther. Author manuscript; available in PMC 2016 June 01.

Published in final edited form as:

Mol Cancer Ther. 2015 June ; 14(6): 1346–1353. doi:10.1158/1535-7163.MCT-14-0793.

CDKN2A/p16 loss implicates CDK4 as a therapeutic target in imatinib-resistant dermatofibrosarcoma protuberans

Grant Eilers[1], **Jeffrey T. Czaplinski**[2], **Mark Mayeda**[1], **Nacef Bahri**[1], **Derrick Tao**[1], **Meijun Zhu**[1], **Jason L. Hornick**[1], **Neal I. Lindeman**[1], **Ewa Sicinska**[2], **Andrew J. Wagner**[3], **Jonathan A. Fletcher**[1], and **Adrian Mariño-Enriquez**[1]

[1] Department of Pathology, Brigham and Women's Hospital, Harvard Medical School, Boston, MA.

[2] Center for Molecular Oncologic Pathology, Department of Medical Oncology, Dana-Farber Cancer Institute, Harvard Medical School, Boston, MA.

[3] Center for Sarcoma and Bone Oncology, Department of Medical Oncology, Dana-Farber Cancer Institute, Harvard Medical School, Boston, MA.

Abstract

Dermatofibrosarcoma protuberans (DFSP) is an aggressive PDGFB-dependent cutaneous sarcoma characterized by infiltrative growth and frequent local recurrences. Some DFSP progress to a higher-grade fibrosarcomatous form, with rapid growth and increased risk of metastasis. Imatinib provides clinical benefit in ~50% of patients with unresectable or metastatic DFSP. However, efficacious medical therapies have not been developed for imatinib-resistant DFSP. We established a model of imatinib-resistant DFSP, and evaluated CDK4/6 inhibition as a genomically-credentialed targeted therapy. DFSP105, an imatinib-resistant human cell line, was established from a fibrosarcomatous DFSP (FS-DFSP), and was studied by SNP arrays and sequencing to identify targetable genomic alterations. Findings were validated *in vitro* and *in vivo*, and confirmed in a series including 12 DFSP and 6 FS-DFSP. SNP analysis of DFSP105 revealed a homozygous deletion encompassing *CDKN2A* and *CDKN2B*. The resultant p16 loss implicated CDK4/6 as a potential therapeutic target in DFSP. We further demonstrated *CDKN2A* homozygous deletion in 1/12 conventional DFSP and 2/6 FS-DFSP, while p16 expression was lost in 4/18 DFSP. *In vitro* treatment of DFSP105 with two structurally distinct selective CDK4/6 inhibitors, PD-0332991 and LEE011, led to inhibition of RB1 phosphorylation and inhibition of proliferation (GI_{50} 160nM and 276nM, respectively). *In vivo* treatment of DFSP105 with PD-0332991 (150mg/kg) inhibited xenograft growth in mice, in comparison with imatinib-treated or untreated tumors. In conclusion, *CDKN2A* deletion can contribute to DFSP progression. CDK4/6 inhibition is a preclinically effective treatment against p16-negative, imatinib-resistant FS-DFSP, and should be evaluated as a therapeutic strategy in patients with unresectable or metastatic imatinib-resistant DFSP.

Correspondence to: Jonathan A. Fletcher, Department of Pathology, Brigham and Women's Hospital, 75 Francis Street, Boston, MA, 02115, jfletcher@partners.org, Telephone: 617-732-7883, Adrian Mariño-Enriquez, Department of Pathology, Brigham and Women's Hospital, 75 Francis Street, Boston, MA, 02115, admarino@partners.org, Telephone: 617-732-8347.

Potential Conflicts of Interest: A. J.Wagner is a consultant/advisory board member for Novartis. Other authors have no conflicts of interest to declare.

Keywords

CDK4; CDKN2A; p16; DFSP; sarcoma

INTRODUCTION

Dermatofibrosarcoma protuberans (DFSP) is a cutaneous spindle cell sarcoma of presumed fibroblastic lineage characterized by an infiltrative growth pattern and high rate of local recurrence [1]. Biologically, DFSP is characterized by a genomic rearrangement involving chromosomes 17 and 22, often in a supernumerary ring chromosome, and less often as the result of the reciprocal balanced translocation t(17;22)(q22;q13) [2-5]. Such rearrangements result in the genetic fusion of *COL1A1* and *PDGFB* [6], placing *PDGFB* under the control of the constitutively active *COL1A1* promoter, and leading to overexpression of PDGFB (platelet-derived growth factor beta) and sustained PDGF receptor signaling due to an activating autocrine loop [7]. Tyrosine kinase inhibitors, such as imatinib, disrupt this autocrine loop by blocking PDGF receptor activity [8]. An estimated 10-20% of DFSP undergo transformation to a higher-grade form, designated fibrosarcomatous DFSP (FS-DFSP) [9-12], which is characterized by rapid growth and increased risk for metastasis [9, 13-16]. The biological mechanisms causing transformation from conventional DFSP to FS-DFSP are not well understood [17]. Therefore, biomarkers that predict tumor progression might be helpful in assessing prognosis and generating new therapeutic leads in patients with DFSP.

Sensitivity to imatinib has been observed both in patients with advanced localized DFSP, as well as metastatic FS-DFSP [18]. However, imatinib response rates barely surpass 50% [12, 18-22]. Many patients do not respond to imatinib [23], and even among those patients who do respond, secondary resistance often emerges rapidly [22, 24]. Biological mechanisms of resistance to imatinib are not well characterized in DFSP, and there are no therapies available for patients with imatinib-resistant tumors, other than aggressive surgical resection that can cause significant morbidity and is an ineffective means for controlling disseminated disease.

For the studies reported herein, we established an imatinib-resistant FS-DFSP cell line, in which we identified a localized homozygous deletion of the *CDKN2A* locus, associated with loss of p16 expression, which suggested tumor dependency on CDK4/6. We then screened a series of conventional DFSP and FS-DFSP, showing that *CDKN2A* deletion and p16 loss are recurrent aberrations in DFSP. Targeting CDK4/6 with specific pharmacological inhibitors decreased DFSP proliferation *in vitro* and tumor growth *in vivo*, thereby validating a novel therapeutic strategy in DFSP.

MATERIALS AND METHODS

Tumor samples

Formalin-fixed, paraffin-embedded tumor samples from 13 conventional and 9 FS-DFSP were obtained from the pathology archives at Brigham and Women's Hospital (**Table 1**).

Two sequential samples, obtained 3 months to 3 years apart, were available for patients DFSP-12, FS-DFSP-03, FSDFSP-05, and FS-DFSP-06. H&E-stained slides were reviewed by two experienced surgical pathologists, confirming the diagnosis of DFSP or FS-DFSP in all cases. Histologically, DFSP is a dermal storiform proliferation of bland spindle cells set in a collagenous matrix without significant cytologic atypia, characteristically extending into subcutaneous fat in a honeycomb pattern. FS-DFSP shows a fascicular arrangement with a herringbone appearance, more cellularity than conventional DFSP, mild nuclear atypia and hyperchromasia, and high mitotic activity (10–20 mitoses per 10 hpf). One of the conventional DFPS had a giant-cell fibroblastoma histomorphology. Where available, snap frozen tissue was collected after surgical resection at Brigham and Women's Hospital. All samples were collected with institutional review board approval.

Index case and cell lines

We established the spontaneously immortal human DFSP cell line, DFSP105, from a right breast axillary tail FS-DFSP metastasis in a 53 year old female. The DFSP had been diagnosed five years earlier, at which time the patient presented with FS-DFSP on the upper back that was resected, but recurred locally shortly after. The diagnosis was molecularly confirmed by *PDGFB* FISH. Lung and bone metastases were also detected at that point and imatinib treatment was started, achieving a PET radiographic response in both the lung and bone lesions. After 10 months on imatinib, the tumor progressed and the patient was later enrolled in a clinical trial of a PI3K inhibitor. The DFSP105 cell line was established from a biopsy of a breast metastasis that arose during the course of this study. At progression, the patient received imatinib in combination with off-label sirolimus, with good initial response discontinued due to thrombotic microangiopathy and renal dysfunction. She subsequently received sunitinib and other investigational agents, but eventually died from disease 6 years after initial diagnosis.

DFSP105 cells were maintained in Iscove's Modified Dulbecco's Medium supplemented with 15% fetal bovine serum, penicillin/streptomycin and 1% (v/v) L-glutamine. The cell line was periodically validated by detection of *PDGFB* rearrangement by FISH. All of the experiments in this report were performed on passage numbers 10-30. Formalin-fixed, paraffin-embedded tissue from this patient's DFSP was included in the study as case FS-DFSP-06. GIST48 and GIST882, previously published gastrointestinal stromal tumor cell lines developed in our laboratory, were used as controls for *in vitro* assays [25].

Fluorescence *In Situ* Hybridization (FISH)

PDGFB FISH was performed according to a standard protocol, as described previously [26]. FISH probes flanking *PDGFB* were RP11-348I7 and RP11-1149B8 (3', centromeric) and RP11-434E5 and RP11-101B10 (5', telomeric). A normal *PDGFB* locus was defined as paired 5' and 3' FISH signals, less than 3 signal widths apart. Cases were considered to have *PDGFB* rearrangement if the 5' and 3' FISH signals were split apart. Vysis LSI *CDKN2A* SpectrumOrange/CEP 9 SpectrumGreen probes (Abbott Molecular) were used for evaluation of the *CDKN2A* locus. At least 50 nuclei were evaluated for each case; those with greater than 30% of nuclei showing chromosome 9 centromere signals but lacking a *CDKN2A* hybridization signal were considered to be positive for *CDKN2A* deletion.

Single nucleotide polymorphism analysis (SNP)

High molecular weight genomic DNA was isolated from DFSP105 using the QIAamp DNA Mini Kit (QIAGEN). DNA was digested with *Nsp*1, and linkers were ligated to the restriction fragments to permit PCR amplification. The PCR products were purified and fragmented by treatment with DNase I, then labeled and hybridized to an Affymetrix 250K SNP array. Signal positions and intensities were analyzed using dChip software. Array intensity was normalized to the array with median intensity. Median smoothing was used to infer copy number.

Massively parallel targeted sequencing

We sequenced a preselected set of 275 cancer-associated genes (OncoPanel), which emphasizes clinically actionable genes, including genes with roles in PDGFR signaling (such as *PDGFRB* and members of the PI3K/AKT/MTOR, RAS/RAF/ERK and PKC signaling pathways) and other cancer-related genes, as previously published [27]. Sample preparation, size selection, capture to biotinylated baits, paired-end sequencing on HiSeq 2000 (Illumina, San Diego, CA), and analytical pipeline have also been described previously [27].

Western Blotting Analysis

Frozen tumor samples were diced in ice-cold lysis buffer containing protease inhibitors and homogenized for 3 seconds, 3-5 times, on ice. Whole-cell lysates from cell cultures were prepared in lysis buffer. All lysates were cleared by centrifugation at 14,000 rpm for 30 min at 4°C, and protein concentrations were determined using a Bradford protein assay (Bio-Rad Laboratories). Electrophoresis, western blotting and detection were performed using standard techniques.

Primary antibodies were p16 (Cell Signaling #4824), phospho-RB1 Ser795 (Cell Signaling #9301), phospho-RB1 Ser807/811 (Cell Signaling #9308), RB (Cell Signaling #9309), CDK4 (Santa Cruz sc-601), PDGFRB (Santa Cruz, sc-432), phospho-PDGFR (sc-12911), actin (Sigma A4700), Cyclin A (Novocastra NCL-CYCLIN A), and Cyclin D1 (Santa Cruz sc-220044). GIST48, which harbors a homozygous *CDKN2A* deletion and expresses no p16, and GIST882, which retains wild type *CDKN2A* and expresses p16, were used as controls for p16 staining.

Drug response studies

Cell proliferation was measured by BrdU incorporation, using a cell proliferation ELISA kit (Roche). Cells were plated at 2500 cells per well in opaque 96-well flat-bottom plates and drugs were added with fresh media 24 hours after plating. Cells were incubated in drug for 48 hours, with BrdU added to the media for the last 24 hours. Luminescence was detected using a Veritas microplate luminometer (Turner Biosystems). The drugs were imatinib, sunitinib, RAD001 (everolimus) and GDC-0941 (all from LC laboratories); and PD-0332991 (palbociclib) and LEE011 (from ChemieTek). All drugs were dissolved in DMSO. DMSO controls were incorporated in all studies, as solvent-only comparators.

CDK4 knockdowns

Lentiviral constructs encoding shRNA-specific sequences targeting *CDK4* transcripts on the pLKO.1puro backbone were selected from the RNAi Consortium (TRC) library (TRCN0000010520: shRNA1; and TRCN0000000363: shRNA2; the TRC website is http://www.broadinstitute.org/rnai/trc/lib). Lentivirus preparations and lentiviral infections were performed as described previously [25]. Cells from 6 well plates were lysed for immunoblot analysis after puromycin selection at 10, 14 and 21 days post-infection; day 14 is shown. Cell proliferation was measured at day 14 after lentiviral infection, by BrdU incorporation over 24h under the same conditions as the drug response studies.

Immunohistochemistry

Immunohistochemistry was performed on 4-um-thick paraffin-embedded tissue sections after pressure cooker antigen retrieval (Biocare Medical; 30 to 40 min at 122ºC) in citrate buffer (Dako Target Retrieval Solution S1699) using mouse monoclonal antibodies anti-Rb (clone G3-245, BD Biosciences, San Diego, CA; 1:100 dilution), anti-p16 (clone E6H4, MTM Labs, Heidelberg, Germany; 1:2 dilution), and anti-CD34 (clone QBEnd10; Dako, Carpinteria, CA; 1:400 dilution). Dako Envision+ Mouse (K4007) secondary antibody was used (30-min incubation at room temperature). The sections were developed using 3,30-diaminobenzidine as substrate and counterstained with Mayer's hematoxylin. Intact expression within the nuclei of endothelial and inflammatory cells served as internal positive controls for p16. Dako mouse IgG1 was used as a negative control. Nuclear staining for RB1 and p16 were scored by two of the authors (G.E. and A.M.E.) as negative (loss of expression) when <10% of cells showed nuclear staining.

Xenograft studies

Mice were maintained, injected and sacrificed in accordance with an approved IACUC protocol at Dana Farber Cancer Institute. Athymic nude mice were injected subcutaneously with 2 million DFSP105 cells suspended in Matrigel (BD Biosciences). After the establishment of tumors (~5 weeks after injection), mice were split into imatinib or PD-0332991 treatment arms. Imatinib was dissolved in water and administered daily at 75 mg/kg by gavage. PD-0332991 was dissolved in a buffer consisting of 10% v/v 0.1M HCl, 10% v/v Cremophor EL (BASF), 20% v/v PEG 300, and 60% v/v acetate buffer, pH 4.6, and administered daily at 150 mg/kg by gavage. No significant weight loss was observed in any of the mice over the experiment period. Tumor volumes were evaluated weekly. After 5 weeks of treatment, mice were given intraperitoneal injections of BrdU, and euthanized 2 hours later by CO_2 inhalation. Tumors were resected, measured, and photographed, lysates were prepared for western blot analysis, and tissue was allocated for histologic examination.

RESULTS

DFSP105 has *COL1A1-PDGFB* fusion but is resistant to imatinib

FISH using probes flanking the *PDGFB* locus showed an abnormal hybridization pattern in the FSDFSP cell line DFSP105 indicative of *PDGFB* rearrangement and low-level copy number gain (3-5 extra copies of an unbalanced split FISH signal) (**Figure 1A**). These

findings are consistent with the ring chromosome demonstrated in DFSP105 by giemsa-banding cytogenetic studies and the clinicopathological diagnosis of FS-DFSP. In drug sensitivity assays, DFSP105 was resistant to imatinib treatment with a GI_{50} value (50% growth inhibition dose) greater than 5μM as measured by ATP-based viability and BrdU-based proliferation assays (**Figure 1B**). Likewise, DFSP105 proliferation was not inhibited by sunitinib, although both imatinib and sunitinib inhibited PDGFRB phosphorylation in DFSP105 cells (**Figure 1C**). DFSP105 growth was only moderately inhibited by the PI3K inhibitor GDC-0941 (GI_{50} >1.5 μM) but remarkably sensitive to the mTOR inhibitor RAD001 (GI_{50}=5nM), indicating continued dependence on pathways downstream of PDGFR (**Figure 1D**). Hence, DFSP105 captures the molecular and clinical characteristics of the patient's tumor, as a convincing model of imatinib-resistant FS-DFSP.

DFSP105 harbors a homozygous *CDKN2A* deletion

Copy number analyses from DFSP105 SNP profiles revealed a localized homozygous deletion at 9p21, encompassing *CDKN2A* and *CDKN2B*, which encode $p14^{ARF}$, $p15^{INK4b}$, and $p16^{INK4a}$ (**Figure 2A**). This was the only homozygous deletion region detected in DFSP105, although there were heterozygous deletions at 4q31-32, 5p13-15, 6q14-27, 17p12-13, 18q12-23, 19q13, and 22q13. Low-level copy number gains were present on 17q and 22q, corresponding to extra copies of the *COL1A1-PDGFB* fusion present in ring chromosomes. Additional low-level copy number gains were present at 5q35, 14q11, 16p11-13, and 16q22. The homozygous *CDKN2A* deletion was confirmed by FISH, which showed no hybridization signals for the *CDKN2A* locus, whereas two signals per cell were demonstrated for the chromosome 9 centromeric region (in both DFSP105 and in sections of the corresponding tumor, FS-DFSP-06). The *CDKN2A* deletion was associated with complete loss of p16 expression, as evaluated by western blot, whereas RB1 expression was retained (**Figure 2B**). Oncopanel sequencing confirmed *CDKN2A* homozygous deletion and also demonstrated a *TP53* frameshift mutation (c.582_588TATCCGA>ATA), allelic frequency ~25%, which was likely present in only a subset of the cells, as well as single nucleotide substitutions in *FH* (c.655G>A, encoding D219N; predicted to be benign - Polyphen2 score 0.0) and *ERCC3* (c.1067C>T, encoding T356I; predicted to be damaging - Polyphen2 score 0.996).

The p16/*CDKN2A*- CDK4-RB1 pathway is frequently disrupted in FS-DFSP

p16 and RB1 expression were analyzed by immunohistochemistry in formalin-fixed paraffin-embedded tissue samples from a series of 18 conventional DFSP and FS-DFSP (**Table 1**). In total, 6 tumors showed loss of either p16 or RB1, in a mutually exclusive manner (2 of 12 conventional DFSP, and 4 of 6 FS-DFSP). 4 tumors had loss of p16 expression (2 conventional DFSP and 2 FS-DFSP) and 2 had loss of RB1 expression (both, FS-DFSP) (**Table 1** and **Figure 3**). Of the 4 tumors with loss of p16 expression, 3 had homozygous *CDKN2A* deletion (2 FS-DFSP and 1 conventional DFSP), whereas the remaining conventional DFSP showed a normal disomic *CDKN2A* FISH pattern. The conventional DFSP with homozygous *CDKN2A* deletion showed hypercellular areas and up to 11 mitoses per 10 high-power fields, but did not meet the criteria for fibrosarcomatous transformation due to the lack of a fascicular growth pattern (**Figure 3, center**). Including

FS-DFSP-06, from which the DFSP105 cell line was derived (**Figure 3, right**), 1 of 12 conventional DFSP and 2 of 6 FS-DFSP harbored homozygous *CDKN2A* deletions, with complete loss of p16 expression.

DFSP105 is sensitive to CDK4/6 inhibition *in vitro* and *in vivo*

Treatment of DFSP105 with the structurally unrelated CDK4/6 inhibitors PD-0332991 and LEE011 for 24 hours inhibited RB1 phosphorylation and inhibited expression of the proliferation marker cyclin A (**Figure 4A**). GI_{50} values for cell proliferation were 160nM for PD-0332991 and 276nM for LEE011 (**Figure 4B**). shRNA-mediated *CDK4* knockdown resulted in substantial inhibition of DFSP105 cell proliferation (**Figure 4C and 4D**). *In vivo* efficacy of CDK4/6 inhibition was evaluated in mouse DFSP105 xenografts, comparing PD-0332991 to PDGF receptor inhibition with imatinib, and to untreated tumors. Growth of DFSP105 xenografts was completely suppressed by PD-0332991, with no detectable increase in tumor size over the treatment period (**Figure 5A**). PD-0332991 significantly reduced DFSP105 xenograft growth compared to no treatment (p=0.0011) and imatinib (p=0.0069), while the growth of imatinib-treated tumors was not significantly different from the untreated controls (p=0.3408). Resected xenografts from mice treated with PD-0332991 showed marked decrease in RB1 phosphorylation (**Figure 5B**). Histologically, the PD-0332991-treated xenografts had similar cell density, with reduced proliferative activity by BrdU incorporation, compared to xenografts from untreated, and imatinib-treated mice (**Figure 5C**).

DISCUSSION

There are few effective therapeutic options for unresectable or metastatic DFSP; although disruption of autocrine PDGF receptor signaling by imatinib has been effective in ~50% of DFSP patients [12, 18-21], the responses are short-lasting and there are no known biomarkers of response. Patients with conventional DFSP often show a good initial response to imatinib, which may enable more effective surgical resection in a neoadjuvant clinical setting [28]. In patients with FS-DFSP, responses to imatinib are often transient, incomplete, and unpredictable [22, 24]. Currently, no effective targeted pharmacologic therapies have been described for patients with imatinib-resistant DFSP [29].

To study genetic progression and imatinib resistance in DFSP, we established a human cell line, DFSP105, from a patient with imatinib-resistant metastatic FS-DFSP. DFSP105 cells expressed tyrosine phosphorylated PDGFRB, consistent with persistent autocrine PDGFB activation from the underlying genomic *COL1A1-PDGFB* rearrangement. However, DFSP105 appeared to be PDGFR-independent, as evidenced by failure of imatinib and sunitinib to inhibit cell proliferation and viability, even though both drugs inhibited PDGFRB phosphorylation (**Figure 1**). Notably, in evaluating potential targets downstream of PDGFRB, we found that DFSP105 proliferation was inhibited potently by mTOR inhibition, whereas anti-proliferative response to the PI3K inhibitor GDC-0941 was less dramatic than that reported in other malignancies with oncogenic PI3K activation [30], suggesting that DFSP105 has partial resistance to this agent. Taken together, these observations suggest continued dependence of DFSP105 on downstream PDGFR signaling,

with a receptor independent imatinib-resistance mechanism. However, targeted sequencing of 275 cancer-related genes did not reveal mutations in genes that regulate mTOR, and are downstream of PI3K, including *AKT* family members, *PTEN*, *TSC1*, *TSC2*, and *MTOR* itself. Hence, the specific molecular mechanism of imatinib-resistance in DFSP105 remains to be pinpointed. The mutations detected in the cancer gene screen were a *TP53* frameshift mutation which appeared to be a late genetic event (likely present in only a subset of the cells), an *FH* mutation predicted to be benign, and an *ERCC3* mutation predicted to be deleterious. None of these mutations have been associated convincingly with acquired resistance to tyrosine kinase inhibitors, and mutations in these genes were not identified by whole genome sequencing in another imatinib-resistant DFSP [31]. Interestingly, it is unclear why a subset of DFSP manifest primary resistance to imatinib, even though they have the same *COL1A1-PDGFB* primary mutation found in patients whose DFSP respond initially to imatinib. In sum, we conclude that the mechanisms of imatinib primary and secondary resistance remain to be identified in DFSP, and the evidence in our study justifies a further focus on candidates downstream of PDGFRB, in the PI3K-mTOR pathway.

SNP analysis of DFSP105 demonstrated a relatively simple genome, notable for a localized 9p21 homozygous deletion, encompassing *CDKN2A* and *CDKN2B*, which encode $p14^{ARF}$, $p15^{INK4b}$, and $p16^{INK4a}$. *CDNK2A* is one of the most frequently altered genes in cancer, and its protein product, p16, acts to restrict cell cycle progression by inhibiting CDK4/6 activity. *CDKN2A* deletion results in constitutive CDK4/6 activity, leading to RB1 hyperphosphorylation and dysregulated cell cycle activity [32, 33]. Cell cycle control in *CDKN2A*-null but RB1-positive tumors can be restored by pharmacological inhibition of CDK4/6 [34]. Phase I and II clinical trials using the highly specific CDK4/6 inhibitor, PD-0332991, have shown promising results in tumors with p16/CDK4 pathway dysregulation [35, 36].

In this study, the selective CDK4/6 inhibitors PD-0332991 and LEE011 inhibited DFSP105 proliferation at GI_{50} doses of 160nM and 276nM, respectively, which are concentrations within the previously reported therapeutic range for other RB1-positive cancer models [34, 37]. These interventions not only inhibited DFSP cell proliferation *in vitro* and tumor growth *in vivo*, but – in keeping with the expected drug mechanisms – inhibited RB1 phosphorylation and inhibited expression of the proliferation marker cyclin A.

To more generally assess the rationale of CDK4 inhibition in DFSP treatment, we queried a series of conventional DFSP and FS-DFSP to determine the frequency of p16 loss in a series of patient samples ranging from treatment-naïve conventional DFSP to imatinib-resistant, metastatic FS-DFSP. Loss of p16 expression and homozygous *CDKN2A* deletion were demonstrated in 22% of cases (4 of 18) including 1 of 12 conventional DFSP and 2 of 6 FS-DFSP. The one conventional DFSP with *CDKN2A* deletion showed hypercellular areas and high mitotic activity, suggesting that *CDKN2A* deletion may serve as a biomarker of tumor progression from DFSP to FS-DFSP, in addition to identifying DFSP with strong rationale for therapeutic CDK4 inhibition.

In summary, we demonstrate *CDKN2A* deletions in a subset of FS-DFSP, and show that CDK4/6 pharmacologic inhibition in FS-DFSP reduces cell proliferation *in vitro* and tumor

burden *in vivo*. These data provide a rationale to clinically evaluate CDK4/6 inhibition as a therapeutic strategy in p16-negative FS-DFSP.

ACKNOWLEDGMENTS

The authors thank Mei Zeng, Alex Anatone and Alexandra Lauria for excellent technical support, as well as Yixiang Zhang and members of the Fletcher Laboratory for useful scientific discussions.

Financial support: This work was supported by grants from the US National Institutes of Health, including 1P50CA168512 (J.A. Fletcher, and A. Mariño-Enriquez) and 1P50CA127003 (J.A. Fletcher), and from The Sarcoma Alliance for Research through Collaboration (A. Mariño-Enriquez).

REFERENCES

1. Gloster HM Jr. Dermatofibrosarcoma protuberans. J Am Acad Dermatol. 1996; 35:375–6.
2. Pedeutour F, Simon MP, Minoletti F, Sozzi G, Pierotti MA, Hecht F, et al. Ring 22 chromosomes in dermatofibrosarcoma protuberans are low-level amplifiers of chromosome 17 and 22 sequences. Cancer Res. 1995; 55:2400–3. [PubMed: 7757993]
3. Naeem R, Lux ML, Huang SF, Naber SP, Corson JM, Fletcher JA. Ring chromosomes in dermatofibrosarcoma protuberans are composed of interspersed sequences from chromosomes 17 and 22. Am J Pathol. 1995; 147:1553–8. [PubMed: 7495279]
4. Pedeutour F, Coindre JM, Nicolo G, Bouchot C, Ayraud N, Carel CT. Ring chromosomes in dermatofibrosarcoma protuberans contain chromosome 17 sequences: Fluorescence in situ hybridization. Cancer Genet Cytogenet. 1993; 67:149. [PubMed: 8330274]
5. Pedeutour F, Simon MP, Minoletti F, Barcelo G, Terrier-Lacombe MJ, Combemale P, et al. Translocation, t(17;22)(q22;q13), in dermatofibrosarcoma protuberans: A new tumor-associated chromosome rearrangement. Cytogenet Cell Genet. 1996; 72:171–4. [PubMed: 8978765]
6. Simon MP, Pedeutour F, Sirvent N, Grosgeorge J, Minoletti F, Coindre JM, et al. Deregulation of the platelet-derived growth factor B-chain gene via fusion with collagen gene COL1A1 in dermatofibrosarcoma protuberans and giant-cell fibroblastoma. Nat Genet. 1997; 15:95–8. [PubMed: 8988177]
7. Shimizu A, O'Brien KP, Sjoblom T, Pietras K, Buchdunger E, Collins VP, et al. The dermatofibrosarcoma protuberans-associated collagen type Ialpha1/platelet-derived growth factor (PDGF) B-chain fusion gene generates a transforming protein that is processed to functional PDGF-BB. Cancer Res. 1999; 59:3719–23. [PubMed: 10446987]
8. Sjoblom T, Shimizu A, O'Brien KP, Pietras K, Dal Cin P, Buchdunger E, et al. Growth inhibition of dermatofibrosarcoma protuberans tumors by the platelet-derived growth factor receptor antagonist STI571 through induction of apoptosis. Cancer Res. 2001; 61:5778–83. [PubMed: 11479215]
9. Bowne WB, Antonescu CR, Leung DH, Katz SC, Hawkins WG, Woodruff JM, et al. Dermatofibrosarcoma protuberans: A clinicopathologic analysis of patients treated and followed at a single institution. Cancer. 2000; 88:2711–20. [PubMed: 10870053]
10. Wrotnowski U, Cooper PH, Shmookler BM. Fibrosarcomatous change in dermatofibrosarcoma protuberans. Am J Surg Pathol. 1988; 12:287–93. [PubMed: 3354755]
11. Connelly JH, Evans HL. Dermatofibrosarcoma protuberans. A clinicopathologic review with emphasis on fibrosarcomatous areas. Am J Surg Pathol. 1992; 16:921–5. [PubMed: 1415902]
12. Llombart B, Monteagudo C, Sanmartin O, Lopez-Guerrero JA, Serra-Guillen C, Poveda A, et al. Dermatofibrosarcoma protuberans: A clinicopathological, immunohistochemical, genetic (COL1A1-PDGFB), and therapeutic study of low-grade versus high-grade (fibrosarcomatous) tumors. J Am Acad Dermatol. 2011; 65:564–75. [PubMed: 21570152]
13. Mentzel T, Beham A, Katenkamp D, Dei Tos AP, Fletcher CD. Fibrosarcomatous ("high-grade") dermatofibrosarcoma protuberans: Clinicopathologic and immunohistochemical study of a series of 41 cases with emphasis on prognostic significance. Am J Surg Pathol. 1998; 22:576–87. [PubMed: 9591728]

14. Diaz-Cascajo C, Weyers W, Borrego L, Inarrea JB, Borghi S. Dermatofibrosarcoma protuberans with fibrosarcomatous areas: A clinico-pathologic and immunohistochemic study in four cases. Am J Dermatopathol. 1997; 19:562–7. [PubMed: 9415611]
15. Abbott JJ, Oliveira AM, Nascimento AG. The prognostic significance of fibrosarcomatous transformation in dermatofibrosarcoma protuberans. Am J Surg Pathol. 2006; 30:436–43. [PubMed: 16625088]
16. Voth H, Landsberg J, Hinz T, Wenzel J, Bieber T, Reinhard G, et al. Management of dermatofibrosarcoma protuberans with fibrosarcomatous transformation: An evidence-based review of the literature. J Eur Acad Dermatol Venereol. 2011; 25:1385–91. [PubMed: 21645124]
17. Abbott JJ, Erickson-Johnson M, Wang X, Nascimento AG, Oliveira AM. Gains of COL1A1-PDGFB genomic copies occur in fibrosarcomatous transformation of dermatofibrosarcoma protuberans. Mod Pathol. 2006; 19:1512–8. [PubMed: 16980946]
18. Heinrich MC, Joensuu H, Demetri GD, Corless CL, Apperley J, Fletcher JA, et al. Phase II, Open-Label Study Evaluating the Activity of Imatinib in Treating Life-Threatening Malignancies Known to Be Associated with Imatinib-Sensitive Tyrosine Kinases. Clin Cancer Res. 2008; 14:2717–25. [PubMed: 18451237]
19. Rutkowski P, Van Glabbeke M, Rankin CJ, Ruka W, Rubin BP, Debiec-Rychter M, et al. Imatinib mesylate in advanced dermatofibrosarcoma protuberans: Pooled analysis of two phase II clinical trials. J Clin Oncol. 2010; 28:1772–9. [PubMed: 20194851]
20. Rutkowski P, Debiec-Rychter M, Nowecki Z, Michej W, Symonides M, Ptaszynski K, et al. Treatment of advanced dermatofibrosarcoma protuberans with imatinib mesylate with or without surgical resection. J Eur Acad Dermatol Venereol. 2011; 25:264–70. [PubMed: 20569296]
21. Kerob D, Porcher R, Verola O, Dalle S, Maubec E, Aubin F, et al. Imatinib mesylate as a preoperative therapy in dermatofibrosarcoma: Results of a multicenter phase II study on 25 patients. Clin Cancer Res. 2010; 16:3288–95. [PubMed: 20439456]
22. Stacchiotti S, Pedeutour F, Negri T, Conca E, Marrari A, Palassini E, et al. Dermatofibrosarcoma protuberans-derived fibrosarcoma: Clinical history, biological profile and sensitivity to imatinib. Int J Cancer. 2011; 129:1761–72. [PubMed: 21128251]
23. McArthur GA, Demetri GD, van Oosterom A, Heinrich MC, Debiec-Rychter M, Corless CL, et al. Molecular and clinical analysis of locally advanced dermatofibrosarcoma protuberans treated with imatinib: Imatinib target exploration consortium study B2225. J Clin Oncol. 2005; 23:866–73. [PubMed: 15681532]
24. Maki RG, Awan RA, Dixon RH, Jhanwar S, Antonescu CR. Differential sensitivity to imatinib of 2 patients with metastatic sarcoma arising from dermatofibrosarcoma protuberans. Int J Cancer. 2002; 100:623–6. [PubMed: 12209598]
25. Marino-Enriquez A, Ou WB, Cowley G, Luo B, Jonker AH, Mayeda M, et al. Genome-wide functional screening identifies CDC37 as a crucial HSP90-cofactor for KIT oncogenic expression in gastrointestinal stromal tumors. Oncogene. 2014; 33:1872–6. [PubMed: 23584476]
26. Labropoulos SV, Fletcher JA, Oliveira AM, Papadopoulos S, Razis ED. Sustained complete remission of metastatic dermatofibrosarcoma protuberans with imatinib mesylate. Anticancer Drugs. 2005; 16:461–6. [PubMed: 15746584]
27. Brastianos PK, Horowitz PM, Santagata S, Jones RT, McKenna A, Getz G, et al. Genomic sequencing of meningiomas identifies oncogenic SMO and AKT1 mutations. Nat Genet. 2013; 45:285–9. [PubMed: 23334667]
28. Ugurel S, Mentzel T, Utikal J, Helmbold P, Mohr P, Pfohler C, et al. Neo-adjuvant imatinib in advanced primary or locally recurrent dermatofibrosarcoma protuberans: A multicenter phase-II DeCOG trial with long-term follow-up. Clin Cancer Res. 2014; 20:499–510. [PubMed: 24173542]
29. Erdem O, Wyatt AJ, Lin E, Wang X, Prieto VG. Dermatofibrosarcoma protuberans treated with wide local excision and followed at a cancer hospital: Prognostic significance of clinicopathologic variables. Am J Dermatopathol. 2012; 34:24–34. [PubMed: 21785324]
30. Raynaud FI, Eccles SA, Patel S, Alix S, Box G, Chuckowree I, et al. Biological properties of potent inhibitors of class I phosphatidylinositide 3-kinases: from PI-103 through PI-540, PI-620 to the oral agent GDC-0941. Mol Can Ther. 2009; 8:1725–38.

31. Hong JY, Liu X, Mao M, Li M, Choi DI, Kang SW, et al. Genetic aberrations in imatinib-resistant dermatofibrosarcoma protuberans revealed by whole genome sequencing. PLoS One. 2013; 8:e69752. [PubMed: 23922791]

32. Ho A, Dowdy SF. Regulation of G(1) cell-cycle progression by oncogenes and tumor suppressor genes. Curr Opin Genet Dev. 2002; 12:47–52. [PubMed: 11790554]

33. Lundberg AS, Weinberg RA. Functional inactivation of the retinoblastoma protein requires sequential modification by at least two distinct cyclin-cdk complexes. Mol Cell Biol. 1998; 18:753–61. [PubMed: 9447971]

34. Fry DW, Harvey PJ, Keller PR, Elliott WL, Meade M, Trachet E, et al. Specific inhibition of cyclin-dependent kinase 4/6 by PD 0332991 and associated antitumor activity in human tumor xenografts. Mol Cancer Ther. 2004; 3:1427–38. [PubMed: 15542782]

35. Flaherty KT, Lorusso PM, Demichele A, Abramson VG, Courtney R, Randolph SS, et al. Phase I, dose-escalation trial of the oral cyclin-dependent kinase 4/6 inhibitor PD 0332991, administered using a 21-day schedule in patients with advanced cancer. Clin Cancer Res. 2012; 18:568–76. [PubMed: 22090362]

36. Dickson MA, Tap WD, Keohan ML, D'Angelo SP, Gounder MM, Antonescu CR, et al. Phase II trial of the CDK4 inhibitor PD0332991 in patients with advanced CDK4-amplified well-differentiated or dedifferentiated liposarcoma. J Clin Oncol. 2013; 31:2024–8. [PubMed: 23569312]

37. Zhang YX, Sicinska E, Czaplinski JT, Remillard SP, Moss S, Wang Y, et al. Antiproliferative Effects of CDK4/6 Inhibition in CDK4-amplified Human Liposarcoma in vitro and in vivo. Mol Cancer Ther. 2014; 13:2184–93. [PubMed: 25028469]

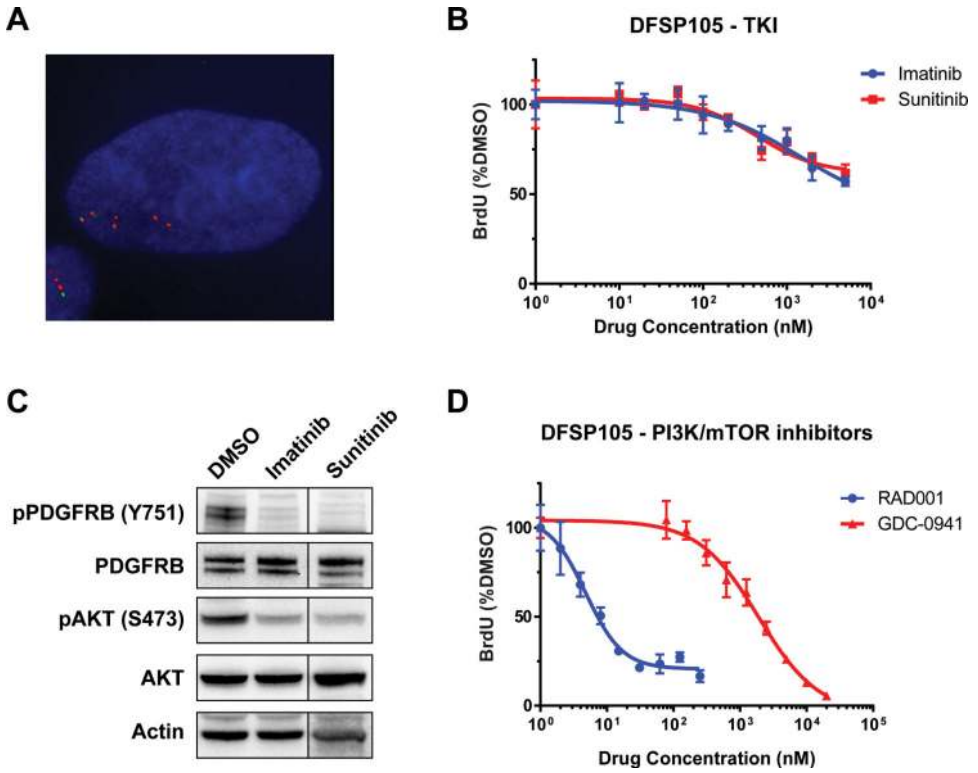

Figure 1.

A. FISH analysis of DFSP105 shows rearrangement and low-level copy number gain of *PDGFB* (3-5 extra copies per cell). Green and red signals correspond to 5' and 3' *PDGFB* probes, respectively. **B**. BrdU-based cell proliferation assay shows DFSP105 resistance to imatinib and sunitinib treatment (GI_{50} > 5μM). **C**. Western blot demonstrates substantial inhibition of PDGFRB tyrosine phosphorylation, with concomitant AKT inhibition, in DFSP105 after treatment with 1 uM imatinib or 500nM sunitinib. **D**. BrdU-based assays show potent DFSP105 anti-proliferative response to mTOR inhibition with RAD001 (GI_{50} = 5 nM), but partial resistance to PI3K inhibition with GDC-0941 (GI_{50} = 1905 nM).

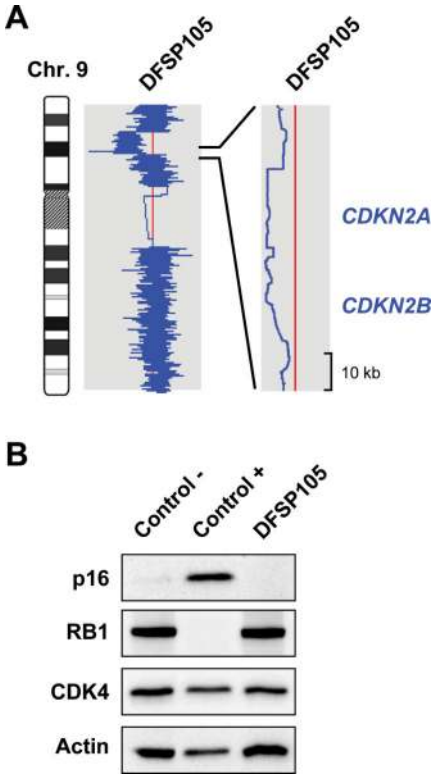

Figure 2.

A. DFSP105 SNP profile for chromosome 9 with detailed view of the 9p21 region, containing *CDKN2A* and *CDKN2B*, on the right. **B**. p16 expression is lost in DFSP105, whereas RB1 expression is retained. Negative and positive controls for p16 staining are GIST48 and GIST882, gastrointestinal stromal tumor cell lines developed in our laboratory with loss of expression of p16 and RB1, respectively.

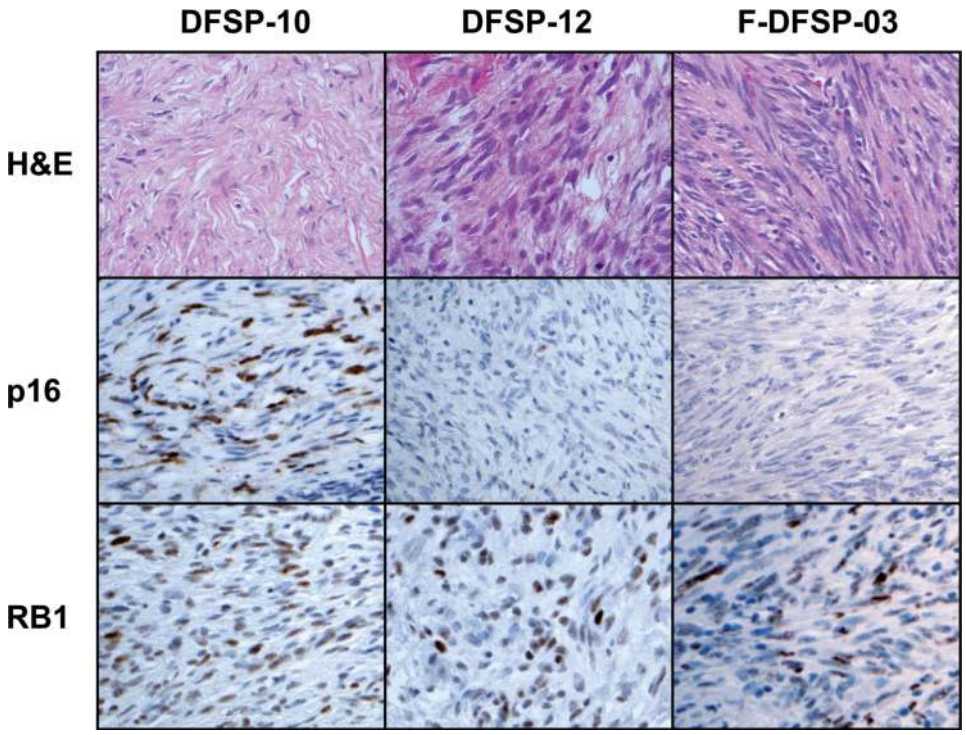

Figure 3.

Representative histologic images of DFSP cases in the study series. **Top**. Hematoxylin and eosin stains, showing conventional DFSP (DFSP-10), a DFSP with increased cellularity and mitotic activity (DFSP-12), and a fibrosarcomatous DFSP with the characteristic fascicular growth pattern (FS-DFSP-03). **Middle**. p16 immunohistochemistry, showing retained p16 expression in DFSP-10 and loss of p16 expression in DFSP-12 and FS-DFSP-03. **Bottom**. RB1 immunohistochemistry, showing retained RB1 expression in cases with p16 loss.

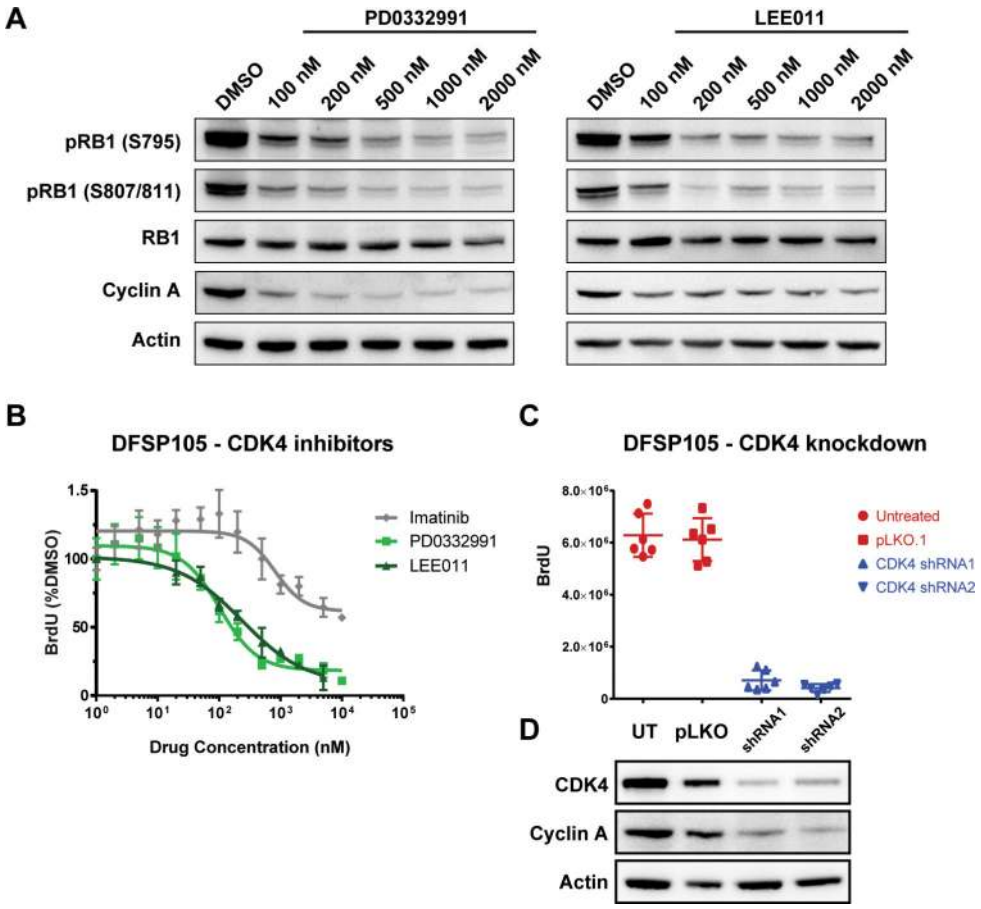

Figure 4.

A. Western blot demonstrates dose-dependent decrease in RB1 phosphorylation and decreased expression of the proliferation marker Cyclin A in DFSP105 after 24h-treatment with the CDK4/6 inhibitors PD-0332991 and LEE011. **B**. Treatments with PD-0332991 and LEE011 inhibit DFSP105 cell proliferation, with GI_{50} of 160nM for PD-0332991 and 276nM for LEE011 as measured by BrdU incorporation. Imatinib response data (from figure 1B) shown for reference. **C**. *CDK4* knockdown by two independent shRNAs resulted in substantial inhibition of DFSP105 cell proliferation as measured by BrdU incorporation. **D**. Western blot confirming *CDK4* knockdown in DFSP105 cells by lentivirally delivered shRNA-1 and shRNA-2, compared with pLKO.1 lentiviral vector and untreated cells.

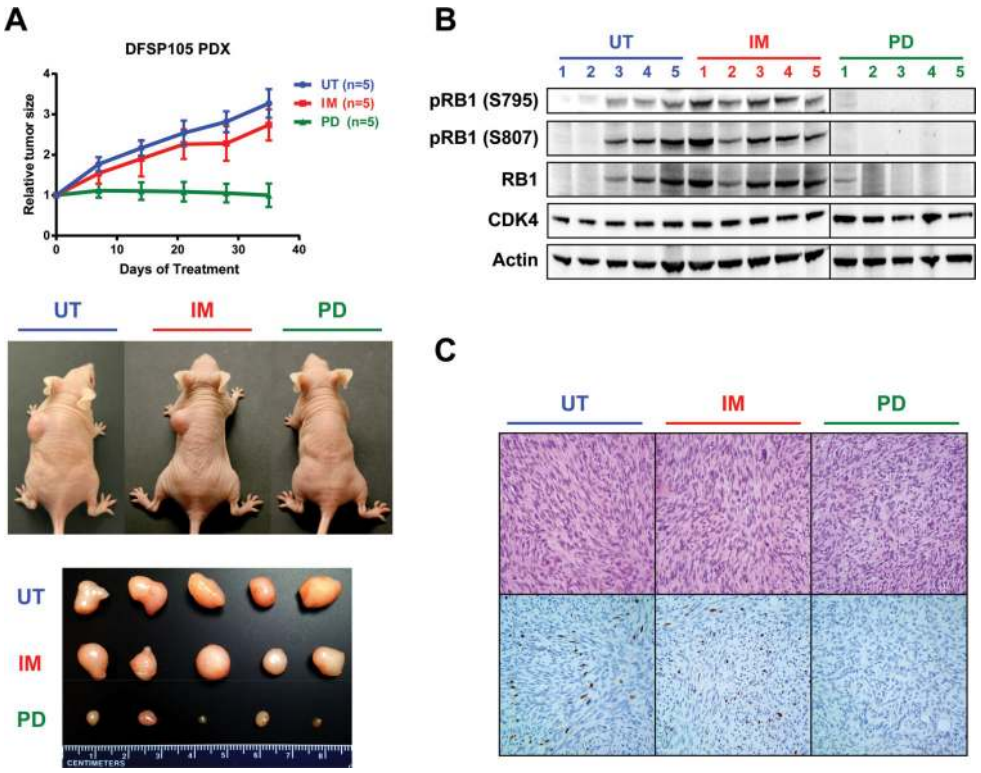

Figure 5.

A. Treatment with PD-0332991 (PD) inhibits growth of DFSP105 xenografts, resulting in a significant decrease (p=0.0391) in tumor size as compared to untreated (UT) and imatinib-treated (IM) controls after 5 weeks of treatment. Data is shown as mean +/- standard error. Images of resected tumors demonstrate the growth inhibitory effect of PD-0332991. **B**. Western blot from whole cell lysates of xenografts treated with PD-0332991 demonstrate marked inhibition of RB1 phosphorylation. **C**. Histologic analysis of resected xenografts demonstrates similar cell density and reduced mitotic activity in PD-0332991-treated tumors compared to imatinib-treated controls. Untreated and imatinib-treated tumors show BrdU incorporation in ~20% of cell nuclei, compared to <1% in the PD-0332991–treated tumors.

Table 1

Clinicopathological features of a series of 18 cases (22 samples) of dermatofibrosarcoma protuberans, including p16/*CDKN2A* status.

Case	Patient ID	Diagnosis[1]	Sex[2] /Age	Location[3]	*PDGFB* FISH[4]	p16 expression[5]	*CDKN2A* FISH[6]	RB1 expression[7]
1	DFSP-01	GCF	M/26	Groin	+	+	+	+
2	DFSP-02	DFSP	M/23	Buttock	+ (2-5)	+	+	+
3	DFSP-03	DFSP	M/34	Forehead	N/A	+	N/A	N/A
4	DFSP-04	DFSP	F/51	Buttock	+ (1-2)	+	+	+
5	DFSP-05	DFSP	F/56	Neck	+ (2-5)	+	+	+
6	DFSP-06	DFSP	F/33	R anterior thigh	-	+	+	+
7	DFSP-07	DFSP	M/27	Forehead	+ (3-5)	-	+	+
8	DFSP-08	DFSP	F/45	Neck / shoulder	+ (3-5)	N/A	+	N/A
9	DFSP-09	DFSP	M/38	Groin	+ (2-4)	+	+	+
10	DFSP-10	DFSP	M/47	Thigh	+ (2-5)	+	+	+
11	DFSP-11	DFSP	F/42	Abdominal wall	+ (1-2)	+	+	+
12	DFSP-12	Hypercellular DFSP	M/55	L anterior chest wall	+ (1-2)	-	Homozygous deletion	+
13	DFSP-12	Hypercellular DFSP	M/55	L anterior chest wall	+ (1-2)	-	Homozygous deletion	+
14	FS-DFSP-01	FS-DFSP	F/75	Chest wall	+ (1-2)	+	+	-
15	FS-DFSP-02	FS-DFSP	F/36	Abdominal wall	+ (1)	+	+	+
16	FS-DFSP-03	FS-DFSP	M/31	L lung metastasis	+	-	Homozygous deletion	+
17	FS-DFSP-03	FS-DFSP	M/34	R lung metastasis	+	-	Homozygous deletion	+
18	FS-DFSP-04	FS-DFSP	M/49	Shoulder	+ (3-5)	+	+	+
19	FS-DFSP-05	FS-DFSP	M/43	Back	+ (3-6)	+	+	-
20	FS-DFSP-05	FS-DFSP	M/44	Back	+ (3-5)	N/A	+	-
21	FS-DFSP-06	FS-DFSP	F/52	R lung metastasis	+	-	Homozygous deletion	+
22*	FS-DFSP-06	FS-DFSP	F/53	R breast metastasis	+ (3-5)	-	Homozygous deletion	+

*This case corresponds to the surgical resection from which the cell line DFSP105 was established.

[1]GCF: Giant cell fibroblastoma; FS-DFSP: fibrosarcomatous DFSP.

[2]M: Male; F: Female

[3]L: left; R: right

[4]Positive/negative (number of copies).

[5]N/A: not available.

[6]N/A: not available.

[7]N/A: not available.